Supplemental Information

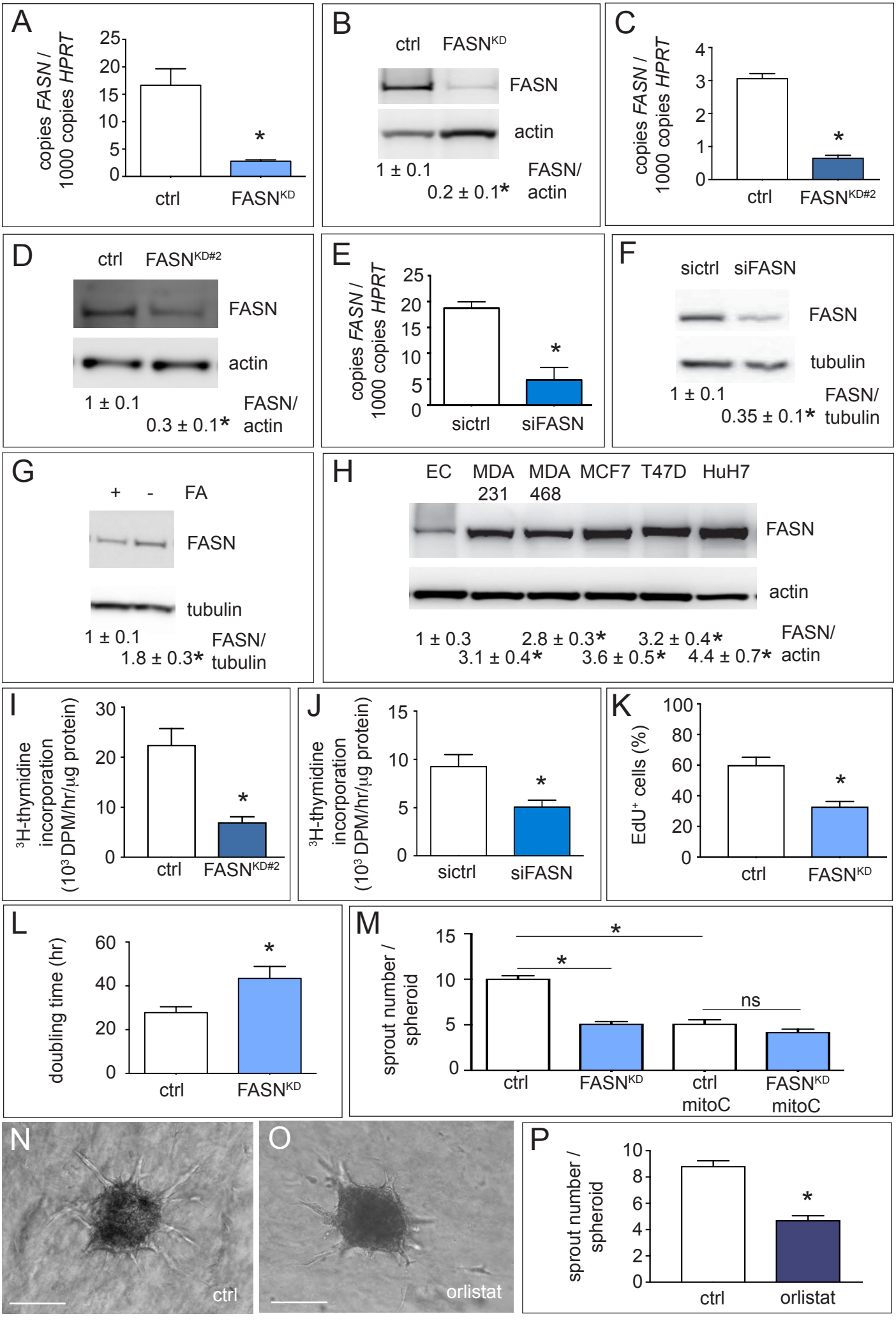
A
copies FASN / 1000 copies HPRT
25
20
15
10
5
0
*
ctrl
FASNKD
B
ctrl
FASNKD
FASN
actin
1 ± 0.1
0.2 ± 0.1*
FASN/ actin
C
copies FASN / 1000 copies HPRT
4
3
2
1
0
*
ctrl
FASNKD#2
D
ctrl
FASNKD#2
FASN
actin
1 ± 0.1
0.3 ± 0.1*
FASN/ actin
E
copies FASN / 1000 copies HPRT
25
20
15
10
5
0
*
sictrl
siFASN
F
sictrl
siFASN
FASN
tubulin
1 ± 0.1
0.35 ± 0.1*
FASN/ tubulin
G
+
-
FA
FASN
tubulin
1 ± 0.1
1.8 ± 0.3*
FASN/ tubulin
H
EC
MDA 231
MDA 468
MCF7
T47D
HuH7
FASN
actin
1 ± 0.3
2.8 ± 0.3*
3.2 ± 0.4*
3.1 ± 0.4*
3.6 ± 0.5*
4.4 ± 0.7*
FASN/ actin
I
3H-thymidine incorporation (10³ DPM/hr/µg protein)
30
20
10
0
*
ctrl
FASNKD#2
J
3H-thymidine incorporation (10³ DPM/hr/µg protein)
15
10
5
0
*
sictrl
siFASN
K
EdU+ cells (%)
100
80
60
40
20
0
*
ctrl
FASNKD
L
doubling time (hr)
60
40
20
0
*
ctrl
FASNKD
M
sprout number / spheroid
15
10
5
0
*
*
ns
ctrl
FASNKD
ctrl mitoC
FASNKD mitoC
N
ctrl
O
orlistat
P
sprout number / spheroid
10
8
6
4
2
0
*
ctrl
orlistat

Figure S1

FIGURE S1 (RELATED TO FIGURE 1): EXPRESSION OF FASN AND EFFECTS OF *FASN* SILENCING ON EC PROLIFERATION AND SPROUTING

(A) *FASN* mRNA levels in control ECs (empty lentiviral vector) and ECs upon *FASN* silencing using a shRNA ($FASN^{KD}$) lentiviral vector (n=7). **(B)** Representative immunoblot of FASN in control and $FASN^{KD}$ ECs. Actin was used as loading control. Densitometric quantification of the FASN to actin ratio, expressed relative to control, is shown beneath the blot (n=6). **(C)** *FASN* mRNA levels in control ECs (empty lentiviral vector) and ECs upon *FASN* silencing using a second non-overlapping shRNA ($FASN^{KD\#2}$) lentiviral vector (n=3). **(D)** Representative immunoblot of FASN in control and $FASN^{KD\#2}$ ECs. Actin was used as loading control. Densitometric quantification of the FASN to actin ratio, expressed relative to control, is shown beneath the blot (n=3). **(E)** *FASN* mRNA levels in control ECs (irrelevant siRNA, sictrl) and in ECs upon *FASN* silencing using a siRNA (siFASN) duplex pool (20 nM) (n=3). **(F)** Representative immunoblot of FASN in sictrl and siFASN ECs. Tubulin was used as loading control. Densitometric quantification of the FASN to tubulin ratio, expressed relative to control, is shown beneath the blot (n=3). **(G)** Representative immunoblot of FASN in ECs, cultured in medium with fatty acids (FA) or without FAs by using charcoal stripped fetal bovine serum. Tubulin was used as loading control. Densitometric quantification of the FASN to tubulin ratio, expressed relative to the FA condition, is shown beneath the blot (n=3). **(H)** Representative immunoblot of FASN in ECs, in the breast cancer cell lines MDA-MB-231 (MDA 231), MDA-MD-468 (MDA 468), MCF7, T47D, and in the hepatocellular carcinoma cell line HuH7. Actin was used as loading control. Densitometric quantification of the FASN to actin ratio, expressed relative to ECs, is shown beneath the blot (n=3). **(I,J)** ^{3}H-thymidine incorporation (proliferation assay) in control and $FASN^{KD\#2}$ ECs (n=3) (I) or in sictrl and siFASN ECs (n=3) (J). DPM, disintegrations per minute. **(K)** Quantification of EdU^{+} ECs after 24 hr EdU labeling in control and $FASN^{KD}$ ECs as measured by flow cytometry (n=3). **(L)** Quantification of doubling time of control and $FASN^{KD}$ ECs (n=3). **(M)** Sprout number per EC spheroid of control and $FASN^{KD}$ EC spheroids with and without mitotic inactivation (mitoC) (n=3). **(N,O)** Representative phase contrast images of EC spheroids cultured with or without the pharmacological FASN blocker (orlistat, 10 µM). Scale bars: 200 µm. **(P)** Sprout number per EC spheroid cultured with or without orlistat. Unless

otherwise indicated, FASN shRNA knockdown experiments were performed using $FASN^{KD\#1}$. Data are mean ± SEM. * $p < 0.05$ by ANOVA (M), mixed models (I,J,K,L,P) or standard two-tailed t test with Welch's correction (all other panel); ns, not significant.

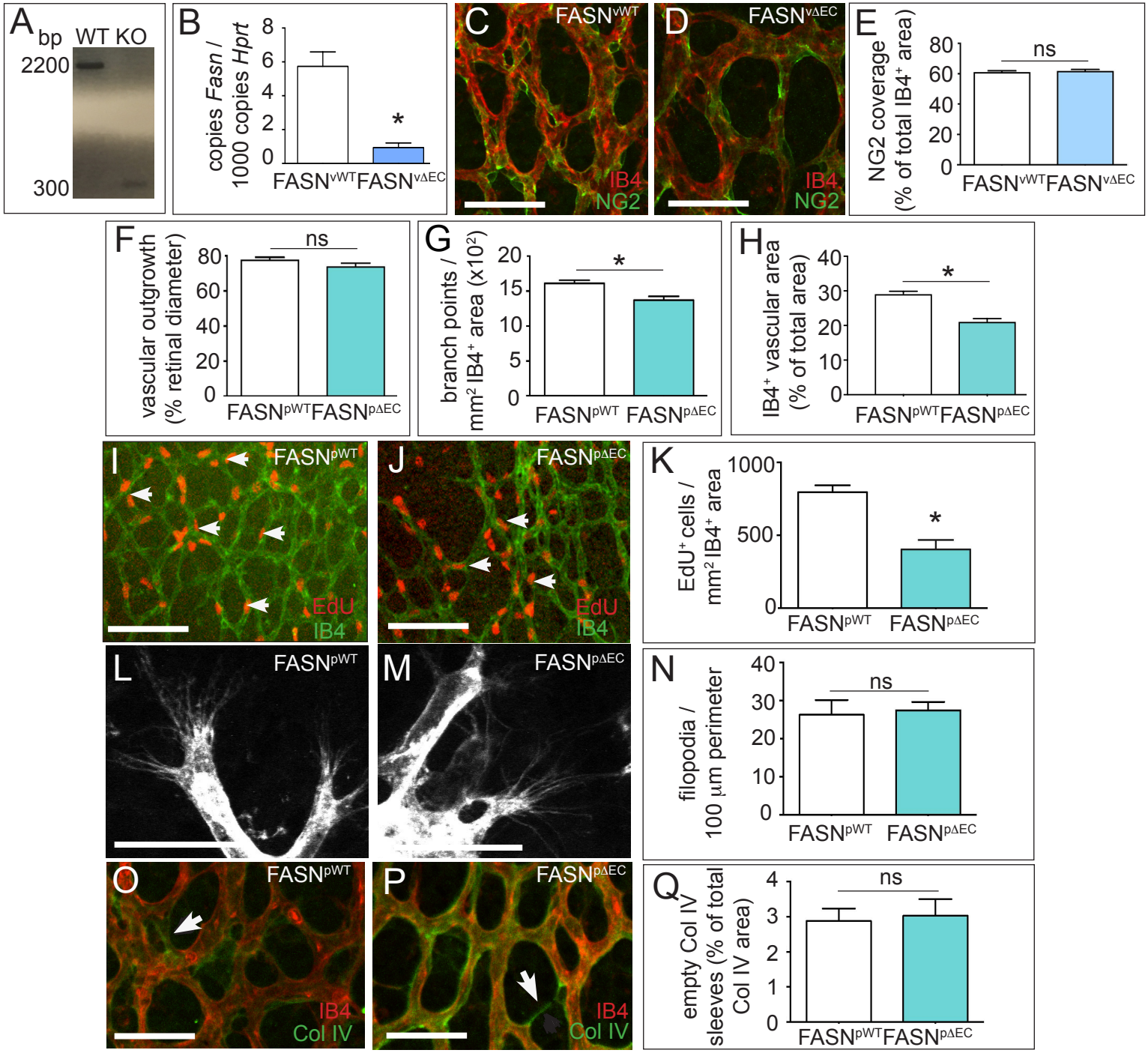
A
bp
WT KO
2200
300
B
copies Fasn / 1000 copies Hprt
8
6
4
2
0
*
FASNvWT FASNvΔEC
C
FASNvWT
IB4
NG2
D
FASNvΔEC
IB4
NG2
E
NG2 coverage (% of total IB4+ area)
80
60
40
20
0
ns
FASNvWT FASNvΔEC
F
vascular outgrowth (% retinal diameter)
80
60
40
20
0
ns
FASNpWT FASNpΔEC
G
branch points / mm2 IB4+ area (x10²)
20
15
10
5
0
*
FASNpWT FASNpΔEC
H
IB4+ vascular area (% of total area)
40
30
20
10
0
*
FASNpWT FASNpΔEC
I
FASNpWT
EdU
IB4
J
FASNpΔEC
EdU
IB4
K
EdU+ cells / mm2 IB4+ area
1000
500
0
*
FASNpWT FASNpΔEC
L
FASNpWT
M
FASNpΔEC
N
filopodia / 100 µm perimeter
40
30
20
10
0
ns
FASNpWT FASNpΔEC
O
FASNpWT
IB4
Col IV
P
FASNpΔEC
IB4
Col IV
Q
empty Col IV sleeves (% of total Col IV area)
4
3
2
1
0
ns
FASNpWT FASNpΔEC

Figure S2

FIGURE S2 (RELATED TO FIGURE 2): EFFECT OF *FASN* LOSS IN ECS ON PHYSIOLOGICAL ANGIOGENESIS *IN VIVO*

(A) Agarose gel image of PCR genotyping of genomic DNA from tamoxifen treated Cre^{-} $FASN^{lox/lox}$ (WT) and Cre^{+} $FASN^{lox/lox}$ (KO) mice showing correct excision of the floxed *Fasn* allele in the Cre^{+} $FASN^{lox/lox}$ mouse, as indicated by the presence of a 300 bp band. **(B)** *Fasn* mRNA levels in ECs isolated from livers of $FASN^{vWT}$ and $FASN^{v\Delta EC}$ mice (respectively Cre negative and Cre positive offspring from intercrosses of VE-Cadherin(PAC)-Cre^{ERT2} mice with $FASN^{lox/lox}$ mice) after tamoxifen injection to induce Cre-activity (n=3 for each genotype). **(C,D)** Representative confocal images of the retinal vasculature of neonatal mice at postnatal day 5 (P5), stained for the pericyte marker NG2 (green) and the EC marker Isolectin-B4 (IB4) (red), in $FASN^{vWT}$ and $FASN^{v\Delta EC}$ mice. Scale bars: 50 µm. **(E)** Quantification of pericyte coverage in $FASN^{vWT}$ (n=5) and $FASN^{v\Delta EC}$ (n=7) neonatal mice. **(F)** Quantification of retinal vascular outgrowth in $FASN^{pWT}$ (n=15) and $FASN^{p\Delta EC}$ (n=18) neonatal mice (respectively Cre negative and Cre positive offspring from intercrosses of PDGFb(PAC)-Cre^{ERT2} mice with $FASN^{lox/lox}$ mice) after tamoxifen injection to induce Cre-activity. **(G)** Number of branch points in the retinal vasculature of $FASN^{pWT}$ (n=15) and $FASN^{p\Delta EC}$ (n=18) neonatal mice. **(H)** Quantification of $IB4^{+}$ retinal vascular area (expressed as % of total area) in $FASN^{pWT}$ (n=7) and $FASN^{p\Delta EC}$ mice (n=7). **(I,J)** Representative confocal images of the retinal vasculature of neonatal mice, stained for EdU (red) and the EC marker IB4 (green), in $FASN^{pWT}$ (I) and $FASN^{p\Delta EC}$ (J) mice. Arrows denote EdU^{+} $IB4^{+}$ ECs. Scale bars: 100 µm. **(K)** Quantification of proliferating EdU^{+} ECs in the retinal vasculature (front of the plexus) of $FASN^{pWT}$ (n=6) and $FASN^{p\Delta EC}$ (n=7) neonatal mice. **(L,M)** Representative high-magnification confocal images of the retinal vascular front (IB4 staining) in $FASN^{pWT}$ (L) and $FASN^{p\Delta EC}$ (M) neonatal mice. Scale bars: 25 µm. **(N)** Number of filopodia per 100 µm perimeter of the retinal vascular front in $FASN^{pWT}$ (n=6) and $FASN^{p\Delta EC}$ (n=7) neonatal mice. **(O,P)** Representative confocal images of the retinal vasculature stained for the EC marker IB4 (red) and the basement membrane marker collagen IV (Col IV) (green), in $FASN^{pWT}$ (O) and $FASN^{p\Delta EC}$) (P) neonatal mice. Arrows indicate isolectin-$B4^{-}$ collagen IV^{+} empty sleeves (green vascular profiles consisting only of green basement membrane without red ECs). Scale bars: 50 µm. **(Q)** Quantification of the percentage of Isolectin-$B4^{-}$ collagen IV^{+} empty sleeves compared to the total collagen IV^{+} vascular area in $FASN^{pWT}$ (n=8) and $FASN^{p\Delta EC}$ (n=10) neonatal mice. Data are mean ± SEM. * $p < 0.05$ by standard two-tailed t-

test; ns, not significant.

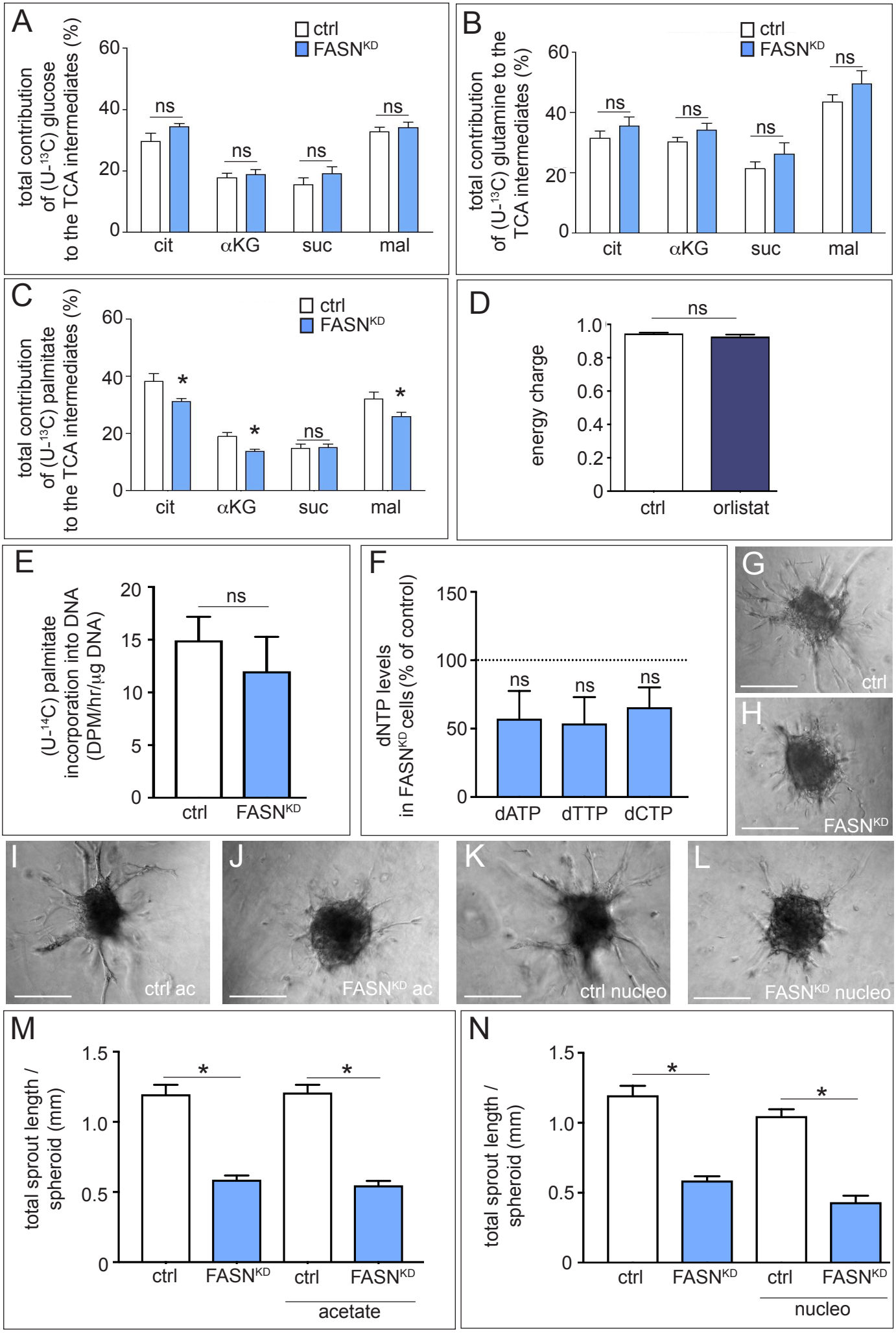
A
total contribution of (U-13C) glucose to the TCA intermediates (%)
ctrl
FASNKD
ns
cit
αKG
suc
mal
B
total contribution of (U-13C) glutamine to the TCA intermediates (%)
C
total contribution of (U-13C) palmitate to the TCA intermediates (%)
*
D
energy charge
ctrl
orlistat
E
(U-14C) palmitate incorporation into DNA (DPM/hr/μg DNA)
F
dNTP levels in FASNKD cells (% of control)
dATP
dTTP
dCTP
G
ctrl
H
FASNKD
I
ctrl ac
J
FASNKD ac
K
ctrl nucleo
L
FASNKD nucleo
M
total sprout length / spheroid (mm)
acetate
N
nucleo

Figure S3

FIGURE S3 (RELATED TO FIGURE 3): EFFECT OF *FASN* SILENCING ON EC METABOLISM

(A-C) ^{13}C tracing analysis of the total contribution of ^{13}C carbons from glucose (A), glutamine (B) or palmitate (C) to the TCA intermediates citrate (cit), α-ketoglutarate (αKG), succinate (suc) and malate (mal) in control and $FASN^{KD}$ ECs (n=3). **(D)** Effect of FASN blockade in ECs using orlistat (10 µM) on energy charge (([ATP] + 1/2 [ADP]) / ([ATP] + [ADP] + [AMP])) (n=3). **(E)** ^{14}C-palmitate incorporation into DNA in control and $FASN^{KD}$ ECs (n=6). DPM, disintegrations per minute. Label incorporation from [U-^{14}C]-palmitate into DNA was not altered by $FASN^{KD}$ likely because the reduction in FAO (see Fig. 3D) was insufficient to impair DNA synthesis (an EC proliferation defect caused by impaired DNA synthesis only occurs when FAO is reduced by 70% (Schoors et al., 2015)). **(F)** dNTP levels in $FASN^{KD}$ ECs compared to control (dashed line) (n=6). **(G,H)** Representative phase contrast images of EC spheroids with control (ctrl) or $FASN^{KD}$ ECs (n=3). Scale bars: 150 µm. **(I,J)** Representative phase contrast images of EC spheroids with control (ctrl) (I) or $FASN^{KD}$ (J) ECs grown in medium supplemented with acetate (ac) (10 mM). Scale bars: 150 µm. **(K,L)** Representative phase contrast images of EC spheroids with control (ctrl) (K) or $FASN^{KD}$ (L) ECs grown in medium supplemented with nucleotides (nucleo) (500 µM per nucleotide). Scale bars: 150 µm. **(M)** Quantification of total sprout length of control (ctrl) and $FASN^{KD}$ spheroids grown in medium without or with supplementation with acetate (10 mM) (n=3). **(N)** Quantification of total sprout length of control (ctrl) and $FASN^{KD}$ spheroids grown in medium without or with supplementation with 500 µM of each nucleotide (nucleo) (n=3). No rescue of the sprouting defect of $FASN^{KD}$ ECs was observed by addition of either acetate or nucleotides to the medium. If the decreased proliferation of $FASN^{KD}$ ECs would be due to a reduction in FAO, then supplementation of acetate (which can be converted to acetyl-CoA in ECs (Schoors et al., 2015)) or nucleotides would be expected to rescue the proliferation defect. Data are mean ± SEM. * $p < 0.05$ by mixed models (A-C), ANOVA (F,M,N) or standard two-tailed t test with Welch's correction (D,E); ns, not significant.

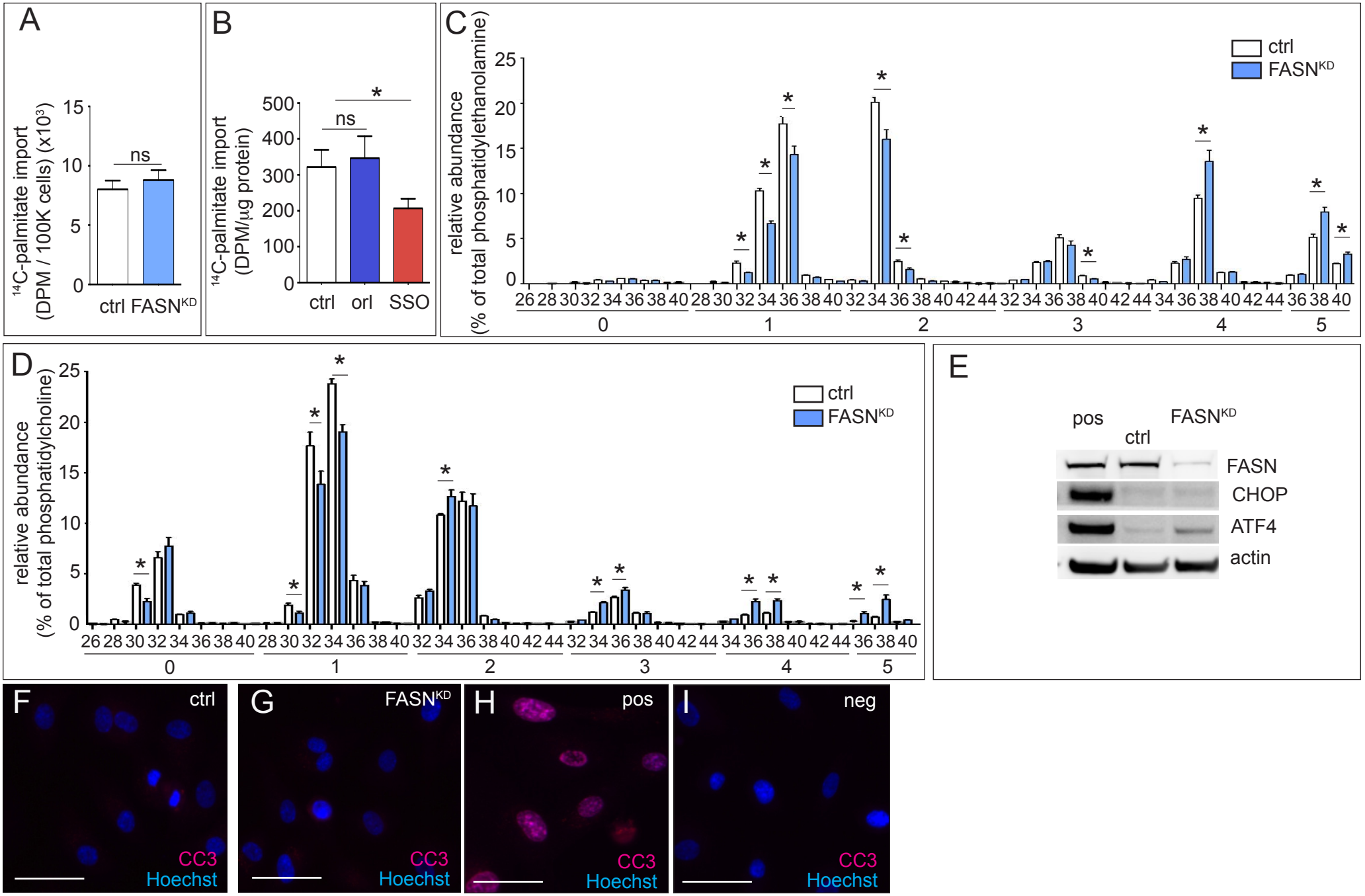
A
^{14}C-palmitate import (DPM / 100K cells) (x10^3)
ns
ctrl FASN^{KD}
B
^{14}C-palmitate import (DPM/μg protein)
ns
*
ctrl orl SSO
C
relative abundance (% of total phosphatidylethanolamine)
ctrl
FASN^{KD}
0 1 2 3 4 5
D
relative abundance (% of total phosphatidylcholine)
ctrl
FASN^{KD}
0 1 2 3 4 5
E
pos
ctrl
FASN^{KD}
FASN
CHOP
ATF4
actin
F
ctrl
CC3
Hoechst
G
FASN^{KD}
CC3
Hoechst
H
pos
CC3
Hoechst
I
neg
CC3
Hoechst

Figure S4

FIGURE S4 (RELATED TO FIGURE 3 AND 4): EFFECT OF *FASN* SILENCING ON PALMITATE LEVELS

(A) Quantification of fatty acid ([U-^{14}C]-palmitate) import in control and FASN^{KD} ECs (n=3). DPM, disintegrations per minute. **(B)** Quantification of fatty acid ([U-^{14}C]-palmitate) import in control, orlistat (orl) or sulfo-N-succinimidyl oleate (SSO) treated ECs (n=3). DPM, disintegrations per minute. **(C,D)** Lipidomic analysis, showing the abundance of saturated, mono-, di- and poly-unsaturated phosphatidyl-ethanolamine (C) and phosphatidylcholine (D) membrane lipids in control and FASN^{KD} ECs (n=3). The numbers under the axes indicate the carbon length of the fatty acid for the different phospholipid species within each group of unsaturation degree (zero to 5). This analysis revealed a moderate decrease in the fraction of mono-unsaturated and increase of poly-unsaturated fatty acyl chains in FASN^{KD} ECs, reflecting reduced palmitate synthesis. In mammalian cells, *de novo* FAS produces saturated fatty acids that can be converted to mono-unsaturated but not to poly-unsaturated species, the latter of which are taken up from the diet (Rysman et al., 2010). Thus, our lipidomics data may suggest that FASN^{KD} ECs display an increased activity of desaturases and/or an increased uptake of poly-unsaturated lipid species. **(E)** Representative immunoblot of ER stress marker CHOP and ATF4 in control and FASN^{KD} ECs. Actin was used as loading control, thapsigargin (200 nM) was used as positive control (pos) (n=4). Despite a moderate increase in ATF4 levels in FASN^{KD} ECs, the protein levels of CHOP (a marker of chronic ER stress and apoptosis) were not elevated by FASN^{KD}. **(F-I)** Representative images of cleaved caspase 3 (CC3) and Hoechst nuclear staining of control (ctrl) (F) and FASN^{KD} ECs (G). Doxorubicin (2 µM) was used as positive (pos) control (H). Negative control was performed without primary antibody for CC3 (neg) (I). Scale bars: 50 µm. Data are mean ± SEM. * $p < 0.05$ by standard two-tailed t-test (C,D), ANOVA (B) or standard two-tailed t test with Welch's correction (A); ns, not significant.

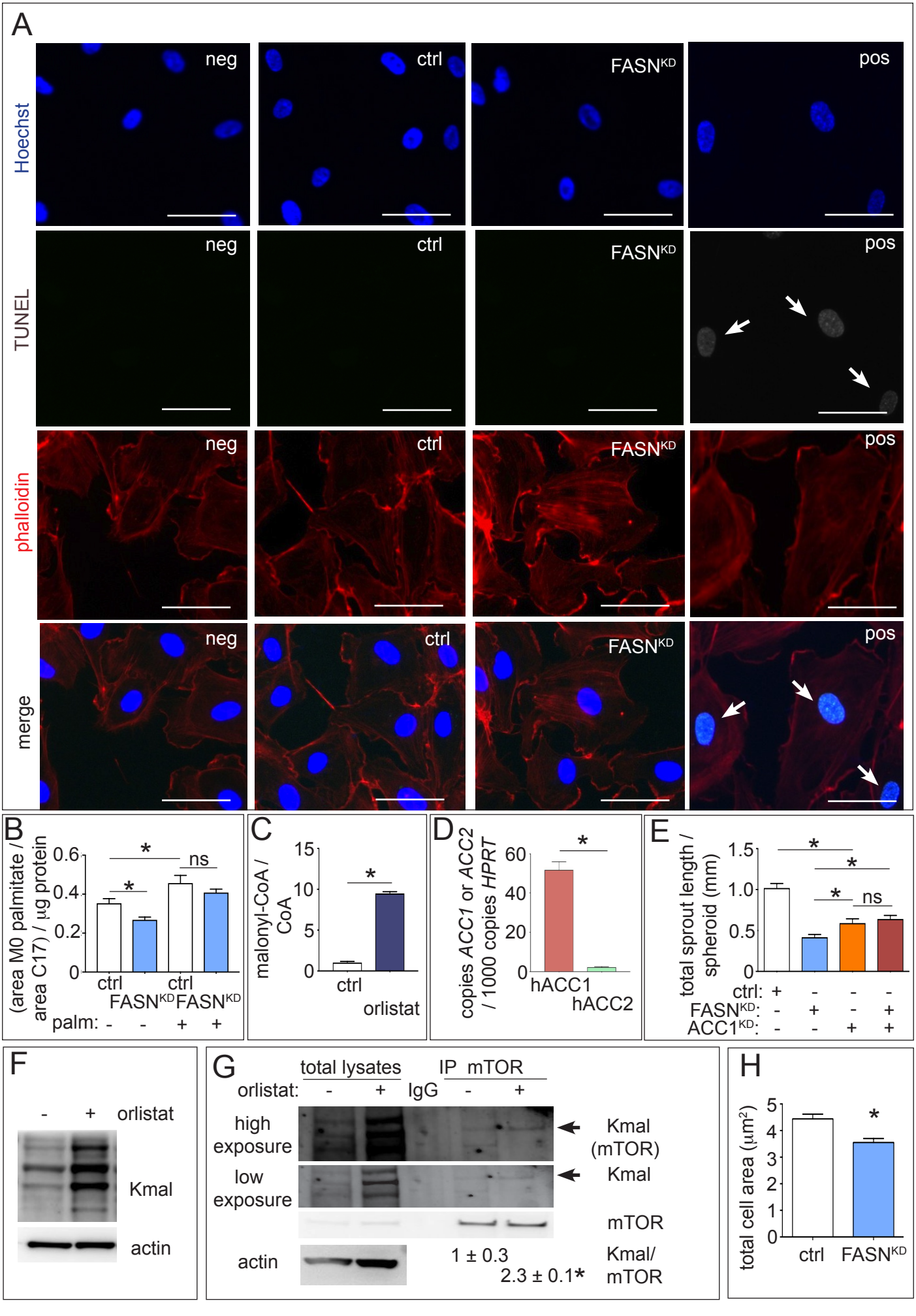
A
Hoechst
TUNEL
phalloidin
merge
neg
ctrl
FASNKD
pos
B
(area M0 palmitate / area C17) / µg protein
ctrl
FASNKD
palm:
ns
C
malonyl-CoA / CoA
orlistat
D
copies ACC1 or ACC2 / 1000 copies HPRT
hACC1
hACC2
E
total sprout length / spheroid (mm)
ctrl:
FASNKD:
ACC1KD:
F
orlistat
Kmal
actin
G
total lysates
IP mTOR
orlistat:
IgG
high exposure
low exposure
Kmal (mTOR)
Kmal
mTOR
actin
1 ± 0.3
2.3 ± 0.1*
Kmal/ mTOR
H
total cell area (µm²)

Figure S5

FIGURE S5 (RELATED TO FIGURE 4 AND 5): EFFECT OF *FASN* OR *ACC1* SILENCING ON MALONYL-COA LEVELS

(A) TUNEL (white in the single signal channel image and green in the merged image), Hoechst nuclear staining (blue) and phalloidin / actin staining (red) of control (ctrl) and $FASN^{KD}$ ECs. Doxorubicin treatment (2 µM) of control ECs was used as positive control (pos), vehicle treatment as negative control (neg). Arrows denote apoptotic cells. EC apoptosis in $FASN^{KD}$ ECs was very rare (precluding meaningful quantitation), suggesting that the activation of the ER stress pathway was insufficient to cause cellular demise. Scale bars: 50 µm. **(B)** Quantification of intracellular palmitate levels (normalized to the standard C17 peak area) in control and $FASN^{KD}$ ECs without or with supplementation with palmitate (palm) (50 µM) (n=3). **(C)** Malonyl-CoA / CoA ratio in control and orlistat treated ECs (n=3). **(D)** Acetyl-CoA carboxylase-1 and -2 (hACC1, hACC2) mRNA expression levels in ECs (n=3). **(E)** Total sprout length in spheroids using control ECs and ECs with single or combined knockdown of *FASN* ($FASN^{KD}$) and *ACC1* ($ACC1^{KD}$) (n=3). **(F)** Representative immunoblot of lysine malonylated (Kmal) proteins in control and orlistat treated ECs. Actin was used as loading control. **(G)** Representative immunoblot of immunoprecipitated (IP) mTOR and immunoblotting for lysine malonylation (Kmal) or mTOR in control and orlistat treated ECs. Actin was used as loading control for total lysates. IgG, negative control for IP. Different exposure images of the blot are shown for visualization of the total lysates (low exposure) and Kmal mTOR (high exposure). Densitometric quantification of the Kmal mTOR to mTOR ratio, expressed relative to untreated ECs, is shown beneath the blot (n=3). **(H)** Quantification of cell size of control and $FASN^{KD}$ ECs, measured on fixed monolayers stained for actin (phalloidin) to visualize cell shape (n=3). Data are mean ± SEM. * $p < 0.05$ by ANOVA (B,E) or standard two-tailed t test with Welch's correction (C,D,G,H); ns, not significant.

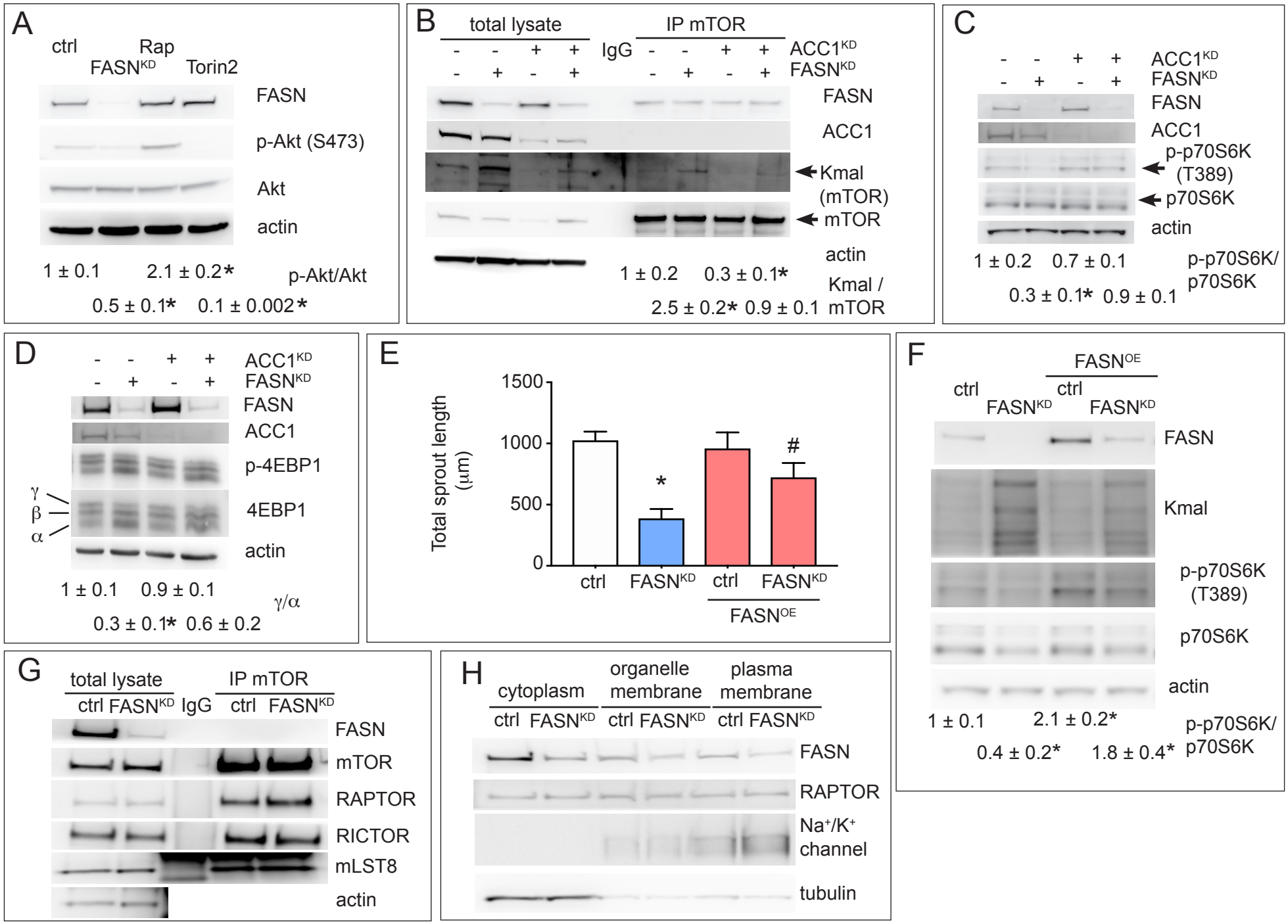
A
ctrl
Rap
FASN^KD
Torin2
FASN
p-Akt (S473)
Akt
actin
1 ± 0.1
2.1 ± 0.2*
p-Akt/Akt
0.5 ± 0.1*
0.1 ± 0.002*
B
total lysate
IP mTOR
IgG
ACC1^KD
FASN^KD
FASN
ACC1
Kmal (mTOR)
mTOR
actin
1 ± 0.2
0.3 ± 0.1*
Kmal / mTOR
2.5 ± 0.2*
0.9 ± 0.1
C
ACC1^KD
FASN^KD
FASN
ACC1
p-p70S6K (T389)
p70S6K
actin
1 ± 0.2
0.7 ± 0.1
p-p70S6K/ p70S6K
0.3 ± 0.1*
0.9 ± 0.1
D
ACC1^KD
FASN^KD
FASN
ACC1
p-4EBP1
γ
β
α
4EBP1
actin
1 ± 0.1
0.9 ± 0.1
γ/α
0.3 ± 0.1*
0.6 ± 0.2
E
Total sprout length (μm)
1500
1000
500
0
*
#
ctrl
FASN^KD
ctrl
FASN^KD
FASN^OE
F
FASN^OE
ctrl
FASN^KD
ctrl
FASN^KD
FASN
Kmal
p-p70S6K (T389)
p70S6K
actin
1 ± 0.1
2.1 ± 0.2*
p-p70S6K/ p70S6K
0.4 ± 0.2*
1.8 ± 0.4*
G
total lysate
IP mTOR
ctrl
FASN^KD
IgG
ctrl
FASN^KD
FASN
mTOR
RAPTOR
RICTOR
mLST8
actin
H
cytoplasm
organelle membrane
plasma membrane
ctrl
FASN^KD
ctrl
FASN^KD
ctrl
FASN^KD
FASN
RAPTOR
Na+/K+ channel
tubulin

Figure S6

FIGURE S6 (RELATED TO FIGURE 5): EFFECT OF *FASN* SILENCING ON MALONYLATION OF MTOR

(A) Representative immunoblot of FASN and of phosphorylated (p-Akt (S473)) and total Akt (downstream target of mTORC2) in control and $FASN^{KD}$ ECs. Actin was used as loading control. The mTORC1 inhibitor rapamycin (Rap) (20 nM) and mTORC1/2 inhibitor Torin2 (100 nM) were used as negative and positive controls, respectively. Densitometric quantification of the p-Akt / Akt ratio, expressed relative to control, is shown beneath the blots (n=3). The FASN and actin shown here are the same as in Fig. 5F, since Akt and 4EBP1 were probed in the same membrane. **(B)** Representative immunoblot of immunoprecipitated (IP) mTOR and immunoblotting for FASN, ACC1, mTOR and lysine malonylation (Kmal) in ECs with single or combined $FASN^{KD}$ and $ACC1^{KD}$. Actin was used as loading control for the total lysates controls (left). IgG, negative control for IP. Densitometric quantification of malonylated mTOR (Kmal/mTOR ratio), expressed relative to non-silenced ECs, is shown beneath the blot (n=3). **(C)** Representative immunoblot of FASN, ACC1, and of total (p70S6K) and phosphorylated (p-p70S6K) downstream target of mTORC1 p70S6K in ECs with single or combined silencing of *FASN* ($FASN^{KD}$) and *ACC1* ($ACC1^{KD}$). Actin was used as loading control. Densitometric quantification of the p-p70S6K / p70S6K ratio, expressed relative to non-silenced ECs, is shown beneath the blots (n=3). **(D)** Representative immunoblot of FASN, ACC1, and of total (4EBP1) and phosphorylated (p-4EBP1) downstream target of mTORC1 4EBP1 in ECs with single or combined silencing of *FASN* ($FASN^{KD}$) and *ACC1* ($ACC1^{KD}$). Actin was used as loading control. Densitometric quantification of the ratio of the high phosphorylated γ to low phosphorylated α form of 4EBP1, expressed relative to non-silenced ECs, is shown beneath the blots (n=3). **(E)** Total sprout length in EC spheroids using control and $FASN^{KD}$ ECs, with or without overexpression of shRNA-resistant *FASN* ($FASN^{OE}$) (n=5). **(F)** Representative immunoblot of FASN, lysine malonylation (Kmal) and of total (p70S6K) and phosphorylated (p-p70S6K) in control and $FASN^{KD}$ ECs, with or without overexpression of *FASN* ($FASN^{OE}$); even though $FASN^{OE}$ was designed to be fully resistant to shRNA-mediated silencing, $FASN^{KD}$ still partially lowered overexpressed FASN levels in $FASN^{OE}$ cells; nonetheless the residual FASN levels in $FASN^{KD}$/$FASN^{OE}$ cells still sufficed to induce a partial rescue. Actin was used as loading control. Densitometric quantification of the p-p70S6K / p70S6K ratio, expressed relative to control ECs, is shown beneath the blots (n=3). **(G)** Representative

immunoblot of immunoprecipitated (IP) mTOR and immunoblotting for FASN, mTOR and co-immunoprecipitated RAPTOR, RICTOR, and mLST8 in control and $FASN^{KD}$ ECs. Actin was used as loading control for the total lysate controls (left). IgG, negative control for IP. **(H)** Representative immunoblot of the cytoplasmic, organelle membrane and plasma membrane protein fraction of total EC lysates, for FASN and RAPTOR (as component of mTORC1) in control and $FASN^{KD}$ ECs. Immunoblotting for tubulin and Na^+/K^+ channel, markers respectively enriched in the cytoplasm and plasma membrane fraction, were included to verify membrane fractionation. Data are mean ± SEM. * $p < 0.05$ versus control (A-F) and # $p < 0.05$ versus $FASN^{KD}$ (E) by standard two-tailed t test with Welch's correction; ns, not significant.

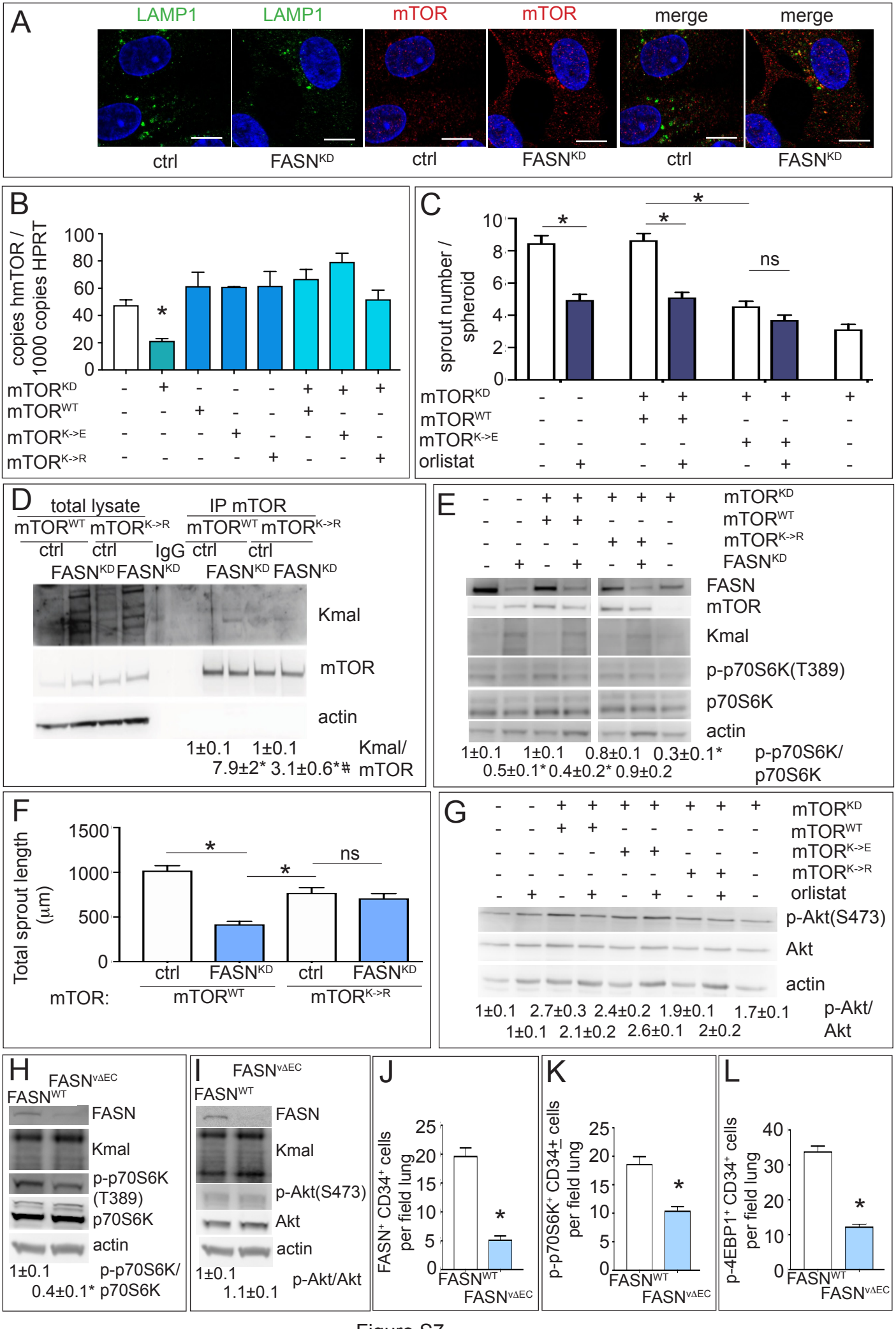
A
LAMP1
LAMP1
mTOR
mTOR
merge
merge
ctrl
FASNKD
ctrl
FASNKD
ctrl
FASNKD
B
copies hmTOR / 1000 copies HPRT
mTORKD
mTORWT
mTORK->E
mTORK->R
C
sprout number / spheroid
ns
mTORKD
mTORWT
mTORK->E
orlistat
D
total lysate
IP mTOR
mTORWT
mTORK->R
ctrl
IgG
FASNKD
Kmal
mTOR
actin
1±0.1 1±0.1 7.9±2* 3.1±0.6*# Kmal/ mTOR
E
mTORKD
mTORWT
mTORK->R
FASNKD
FASN
mTOR
Kmal
p-p70S6K(T389)
p70S6K
actin
1±0.1 1±0.1 0.8±0.1 0.3±0.1* 0.5±0.1* 0.4±0.2* 0.9±0.2 p-p70S6K/ p70S6K
F
Total sprout length (μm)
ns
ctrl
FASNKD
mTOR:
mTORWT
mTORK->R
G
mTORKD
mTORWT
mTORK->E
mTORK->R
orlistat
p-Akt(S473)
Akt
actin
1±0.1 2.7±0.3 2.4±0.2 1.9±0.1 1.7±0.1 1±0.1 2.1±0.2 2.6±0.1 2±0.2 p-Akt/ Akt
H
FASNvΔEC
FASNWT
FASN
Kmal
p-p70S6K (T389)
p70S6K
actin
1±0.1 0.4±0.1* p-p70S6K/ p70S6K
I
FASNvΔEC
FASNWT
FASN
Kmal
p-Akt(S473)
Akt
actin
1±0.1 1.1±0.1 p-Akt/Akt
J
FASN+ CD34+ cells per field lung
FASNWT
FASNvΔEC
K
p-p70S6K+ CD34+ cells per field lung
FASNWT
FASNvΔEC
L
p-4EBP1+ CD34+ cells per field lung
FASNWT
FASNvΔEC

Figure S7

FIGURE S7 (RELATED TO FIGURE 6): ROLE OF LYSINE 1218 IN THE REGULATION OF MTOR ACTIVITY UPON FASN BLOCKADE

(A) Representative immunostaining for the lysosome marker LAMP1 (green), mTOR (red), and Hoechst nuclear (blue) staining of control (ctrl) and $FASN^{KD}$ ECs to assess mTOR localization to the lysosome. Scale bars: 10 µm. **(B)** *mTOR* mRNA expression levels in control ECs and in ECs with single or combined silencing of wild type *mTOR* ($mTOR^{KD}$) and overexpression of a wild-type mTOR construct ($mTOR^{WT}$), an mTOR mutant construct harboring a K1218E ($mTOR^{K->E}$) mutation, or mTOR mutant construct harboring a K1218R ($mTOR^{K->R}$). The $mTOR^{WT}$, $mTOR^{K->E}$, and $mTOR^{K->R}$ constructs are $mTOR^{KD}$ resistant (n=3). **(C)** Sprout number per EC spheroid from spheroids shown in Figure 6G-M, using control and orlistat treated ECs, with single of combined silencing of wild type *mTOR* ($mTOR^{KD}$) and overexpression of a wild type mTOR construct ($mTOR^{WT}$) or an mTOR mutant construct harboring a K1218E ($mTOR^{K->E}$) mutation (n=3). The effects of the $mTOR^{K>E}$ mutant are quantitatively very similar to those of $FASN^{KD}$, which was unexpected given a malonylation stoichiometry of close to 100% for the $mTOR^{K>E}$ mutant while only 4.5% for $FASN^{KD}$. However, the lack of difference may relate to the fact that the glutamic acid mutant is not an absolute accurate model of constitutive malonylation, since it recapitulates the charge change associated with the modification, but not the steric effects of malonylation. **(D)** Representative immunoblotting (IB) of pan-lysine malonylation (Kmal), mTOR, and actin as loading control, of immunoprecipitated (IP) mTOR (right) and the respective total lysates (left) from control or *FASN* silenced ($FASN^{KD}$) ECs, expressing either wildtype *mTOR* ($mTOR^{WT}$) or mTOR harboring a K1218R mutation ($mTOR^{K->R}$, precluding malonylation). IgG, negative control for IP. Densitometric quantification of the malonylated mTOR to total mTOR ratio (Kmal/mTOR), expressed relative to control, is shown beneath the blot. Endogenous *mTOR* was not silenced to avoid overt toxicity owing to high viral load in otherwise triple transduced cells. The residual increase of the Kmal signal in $mTOR^{K->R}$ ECs results from endogenous wild type mTOR (n=3). **(E)** Representative immunoblots of FASN (to check *FASN* silencing), mTOR (to assess mTOR (re-)expression), pan-lysine malonylation (Kmal) (to determine induction of mTOR malonylation upon $FASN^{KD}$), total and phosphorylated p70S6K (mTORC1 target) and actin as loading control, in control and $FASN^{KD}$ ECs silenced for endogenous mTOR ($mTOR^{KD}$) and re-expressing $mTOR^{WT}$, or $mTOR^{K->R}$ (precluding malonylation). Densitometric quantification of p-

p70S6K/p70S6K ratio, expressed relative to control, is shown beneath the blot (n=3). **(F)** Total sprout length in spheroids of control (ctrl) and *FASN* silenced ($FASN^{KD}$) ECs overexpressing wildtype *mTOR* ($mTOR^{WT}$) or $mTOR^{K->R}$ after *mTOR* silencing (n=4). **(G)** Representative immunoblots of total and phosphorylated Akt (mTORC2 downstream target), and actin as loading control, in control and orlistat treated ECs silenced for endogenous mTOR ($mTOR^{KD}$) and re-expressing $mTOR^{WT}$, $mTOR^{K->E}$, or $mTOR^{K->R}$ (n=3). Densitometric quantification of p-Akt/Akt ratio, expressed relative to control, is shown beneath the blot. **(H,I)** Representative immunoblots for FASN (to check *Fasn* KO), pan-lysine malonylation (Kmal, to assess the FASN-KO induction of Kmal), and total and phosphorylated p70S6K (H), or for FASN and total and phosphorylated Akt (I) in murine liver ECs isolated from adult wildtype ($FASN^{WT}$) or endothelial-specific *Fasn* KO ($FASN^{v\Delta EC}$) mice (n=3). Actin was used as loading control. Densitometric quantification of the p-p70S6K/p70S6K (H) or p-Akt/Akt ratios (I), expressed relative to control, is shown beneath each blot. **(J-L)** Quantification of lung sections isolated from $FASN^{WT}$ or $FASN^{v\Delta EC}$ mice, stained for EC marker CD34, and FASN (J) or phosphorylated mTORC1 target p70S6K (p-70S6K) (K) or 4EBP1 (p-4EBP1) (L). The number of $FASN^{+}$ $CD34^{+}$, p-$p70S6K^{+}$ $CD34^{+}$, and p-$4EBP1^{+}$ $CD34^{+}$ cells per field was quantified (n=4). Data are mean ± SEM. * $p < 0.05$ by t-test (panels H-L) or ANOVA (rest of panels).

TABLE S1: MALONYLATED PROTEINS IN FASN SILENCED CELLS THAT HAVE BEEN IDENTIFIED IN PREVIOUS MALONYLATION PEPTIDE SCREENS (RELATED TO FIGURE 5).

Accession [a]	Identifier [a]	Name	Malonylated peptide sequence [b]	Start position [b]	Previous references [c]
Glycolysis and Pentose Phosphate pathway [d]					
P52209	6PGD	6-phosphogluconate dehydrogenase, decarboxylating	TVSKVDDFLANEAK	35	D,C,N
P04075	ALDOA	Fructose-bisphosphate aldolase A	VDKGVVPLAGTNGETTTQGLDGLSER	109	D,C,N
P06733	ENOA	Alpha-enolase	YGKDATNVGDEGGFAPNILENK	200	D,C,N
P04406	G3P	Glyceraldehyde-3-phosphate dehydrogenase	TVDGPSGKLWR	187	D,C,N
			GALQNIIPASTGAAKAVGK	201	
P00558	PGK1	Phosphoglycerate kinase 1	VDFNVPMKNNQITNNQR	23	D,C,N
			ALESPERPFLAILGGAKVADK	200	
P15259	PGAM2	Phosphoglycerate mutase 2	HYGGLTGLNKAETAAK	91	C,D
P14618	KPYM	Pyruvate kinase PKM	GADFLVTEVENGGSLGSKK	189	C, N, D
P29401	TKT	Transketolase	VGDKIATR	311	C, N, D
Cytoskeletal regulation					
P60709	ACTB	Actin, cytoplasmic 1	HQGVMVGMGQKDSYVGDEAQSK	40	D,N
P61160	ARP2	Actin-related protein 2	SEFYKHIVLSGGSTMYPGLPSR	295	C,N
O15143	ARC1B	Actin-related protein 2/3 complex subunit 1B	IFSAYIKEVEERPAPTPWGSK	168	C
P23528	COF1	Cofilin-1	LTGIKHELQANCYEEVK	128	C,N
			HELQANCYEEVKDR	133	
P60660	MYL6	Myosin light polypeptide 6	NKDQGTYEDYVEGLR	80	C
P35579	MYH9	Myosin-9	DDIQKMNPPK	70	C
			HSQAVEELAEQLEQTKR	1194	
P07737	PROF1	Profilin-1	TKSTGGAPTFNVTVTK	90	C, N
			STGGAPTFNVTVTKTDK	92	
Integrin signaling pathway					
P21333	FLNA	Filamin-A	VGTECGNQKVR	570	C
			TGVAVNKPAEFTVDAKHGGK	685	
			GLGLSKAYVGQK	2564	
O75369	FLNB	Filamin-B	APLKIFAQDGEGQR	678	C
Q9Y490	TLN1	Talin-1	TVKAVEDEATK	2131	C,N
Other pathways					
P07108	ACBP	Acyl-CoA-binding protein	TKPSDEEMLFIYGHYK	18	D,C,N
P05141	ADT2	ADP/ATP translocase 2	DFLAGGVAAAISKTAVAPIER	11	D, C
P12236	ADT3	ADP/ATP translocase 3	DFLAGGIAAAISKTAVAPIER	11	C
P04083	ANXA1	Annexin 1	DLAKDITSDTSGDFR	163	C
P07355	ANXA2	Annexin A2	TDLEKDIISDTSGDFR	153	C
P08133	ANXA6	Annexin A6	PANDFNPDADAKALR	359	C, N, D
Q8N3C0	ASCC3	Activating signal cointegrator 1 complex subunit 3	ELTGDMQLSKSEILR	563	C,N,D

O00299	CLIC1	Chloride intracellular channel protein 1	FSAYIKNSNPALNDNLEK	114	C
Q13620	CUL4B	Cullin-4B	GKDIEDGDK	799	C
P04080	CYTB	Cystatin-B	FPVFKAVSFK	35	C
			AKHDELTYF	90	
Q92499	DDX1	ATP-dependent RNA helicase DDX1	TKIDCDNLEQYFIQQGGGPDK	515	C
Q14204	DYHC1	Cytoplasmic dynein 1 heavy chain 1	SFDSEFKLACK	4277	C,N
P68104	EF1A1	Elongation factor 1-alpha 1	EVSTYIKK	173	C, N, D
			LPLQDVYKIGGIGTVPVGR	248	
Q01469	FABP5	Fatty acid-binding protein, epidermal	TESTLKTTQFSCTLGEK	56	C
P14324	FPPS	Farnesyl pyrophosphate synthase	EVLEYNAIGGKYNR	113	C,D
P48506	GSH1	Glutamate--cysteine ligase catalytic subunit	DICKGGNAVVDGCGK	489	D,C,N
P78417	GSTO1	Glutathione S-transferase omega-1	SLGKGSAPPGPVPEGSIR	8	C,N
O60814	H2B1K	Histone H2B type 1-K	LLLPGELAKHAVSEGTK	101	D,C
P17096	HMGA1	High mobility group protein HMG-I/HMG-Y	KQPPVSPGTALVGSQKEPSEVPTPK	31	C
P52272	HNRPM	Heterogeneous nuclear ribonucleoprotein M	GCGVVKFESPEVAER	693	C
P11142	HSP7C	Heat shock cognate 71 kDa protein	NQTAEKEEFEHQQKELEK	584	C, N, D
P04792	HSPB1	Heat shock protein beta-1	DGVVEITGKHEER	115	C
Q14145	KEAP1	Kelch-like ECH-associated protein 1	EQGMEVVSIEGIHPKVMER	117	C
P83111	LACTB	Serine beta-lactamase-like protein LACTB, mitochondrial	KKNDFEQGELYLR	283	D,C,N
P09382	LEG1	Galectin-1	GEVAPDAKSFVLNLGK	22	C
P14174	MIF	Macrophage migration inhibitory factor	SYSKLLCGLLAER	75	C
P42345	MTOR	Serine/threonine-protein kinase mTOR	IVKGYTLADEEEDPLIYQHR	1216	C
P06748	NPM	Nucleophosmin	ADKDYHFKVDNDENEHQLSLR	25	C
A6NDG6	PGP	Phosphoglycolate phosphatase	NNQESDCVSKK	291	C
Q9Y3A3	PHOCN	MOB-like protein phocein	HTLDGAACLLNSNKYFPSR	127	C
P62937	PPIA	Peptidyl-prolyl cis-trans isomerase A	SIYGEKFEDENFILK	77	C, N, D
			TEWLDGKHVVFGK	119	
Q9UMS4	PRP19	Pre-mRNA-processing factor 19	GKTVPEELVKPEELSK	191	C
P25789	PSA4	Proteasome subunit alpha type-4	ATCIGNNSAAAVSMLKQDYK	161	C,N
P61353	RL27	60S ribosomal protein L27	AVIVKNIDDGTSDRPYSHALVAGIDR	23	D,C,N
Q9P2E9	RRBP1	Ribosome-binding protein 1	SKCEELSGLHGQLQEAR	931	C,N
O75396	SC22B	Vesicle-trafficking protein SEC22b	DLQQYQSQAKQLFR	29	C
O00193	SMAP	Small acidic protein	INEELESQYQQSMDSKLSGR	76	C
P49458	SRP09	Signal recognition particle 9 kDa protein	VTDDLVCLVYKTDQAQDVK	42	C
P23381	SYWC	Tryptophan--tRNA ligase, cytoplasmic	MSASDPNSSIFLTDTAKQIK	350	C
P17987	TCPA	T-complex protein 1 subunit alpha	SLHDALCVVKR	391	C, N, D
			DTEPLIQTAKTTLGSK	161	
Q15185	TEBP	Prostaglandin E synthase 3	DVNVNFEKSK	26	C, N
Q9Y277	VDAC3	Voltage-dependent anion-selective channel protein 3	YKVCNYGLTFTQK	62	D,C,N
P08670	VIME	Vimentin	SKFADLSEAANR	293	C

Q8IWA0	WDR75	WD repeat-containing protein 75	SEQPTLVTASKDGYFK	456	C

([a]) For each malonylated protein, the Uniprot accession number and identifier and are indicated.

([b]) Sequence of the peptide containing the modified lysine (red) and the position in the protein sequence of the start residue in the peptide are shown.

([c]) C = Colak et al., 2015; D = Du et al., 2015; N = Nishida et al., 2015.

([d]) Malonylation of glycolytic enzymes can lower their enzymatic activity, as seen in other cell types (Du et al., 2015; Kulkarni et al., 2017; Nishida et al., 2015). In our study, we did not observe a reduction in glycolytic flux in ECs upon FASN inhibition. While the precise reasons remain to be identified, hypothetical non-exclusive explanations include: (i) Cell type-specific differences in the regulation of metabolic pathways (glycolysis); we previously reported that EC metabolism differs from other cell types (De Bock et al., 2013; Schoors et al., 2015) and that ECs are glycolysis-addicted and thus attempt to maintain high glycolysis levels (De Bock et al., 2013), (ii) maintaining glycolysis to compensate for the reduced FAO flux, (iii) insufficient malonylation of glycolytic enzymes (Kulkarni et al., 2017).

TABLE S2: AMINO ACID SEQUENCE CONSERVATION SURROUNDING LYSINE 1218 IN MTOR FOR DIFFERENT SPECIES (RELATED TO FIGURE 6).

Species	Species (latin)	Sequence [a]	Position of the lysine [b]	Validation [c]
Human	*Homo sapiens*	ICRIVKGYTLA	1218	Yes
Mouse	*Mus musculus*	ICRIVKGYTLA	1218	Yes
Rat	*Rattus norvegicus*	ICRIVKGYTLA	1218	Yes
Giant panda	*Ailuropoda melanoleuca*	ICRIVKGYTLA	1218	No
Alligator	*Alligator mississippiensis*	ICRIVKGYTLA	1218	No
Lizard	*Anolis carolinensis*	ICRIVKGYTLA	1219	No
Cattle	*Bos taurus*	ICRIVKGYTLA	1218	No
Dog	*Canis familiaris*	ICRIVKGYTLA	1218	No
Goat	*Capra hircus*	ICRIVKGYTLA	1218	No
Guinea pig	*Cavia porcellus*	ICRIVKGYTLA	1218	No
Green monkey	*Chlorocebus sabaeus*	ICRIVKGYTLA	1218	No
Cat	*Felis catus*	ICRIVKGYTLA	1218	No
Gorilla	*Gorilla gorilla gorilla*	ICRIVKGYTLA	1218	No
Squirrel	*Ictidomys tridecemlineatus*	ICRIVKGYTLA	1218	No
Elephant	*Loxodonta africana*	ICRIVKGYTLA	1218	No
Macaque	*Macaca mulatta*	ICRIVKGYTLA	1218	No
Opossum	*Monodelphis domestica*	ICRIVKGYTLA	1217	No
Ferret	*Mustela putorius furo*	ICRIVKGYTLA	1218	No
Bat	*Myotis lucifugus*	ICRIVKGYTLA	1217	No
Rabbit	*Oryctolagus cuniculus*	ICRIVKGYTLA	1218	No
Galago	*Otolemur garnettii*	ICRIVKGYTLA	1218	No
Sheep	*Ovis aries*	ICRIVKGYTLA	1218	No
Baboon	*Papio anubis*	ICRIVKGYTLA	1217	No
Wild boar	*Sus scrofa*	ICRIVKGYTLA	1218	No

All mTOR amino acid sequences were obtained from Uniprot.

([a]) For each species, the 5 amino acids flanking either side of lysine 1218 are shown.

([b]) In some species (highlighted in blue) the lysine is located on position 1217 or 1219.

([c]) Yes: confirmed expression of mTOR at the protein level. No: putative mTOR protein expression was inferred from genetic sequence homology in those species to human.